Structure-function relationship in photosynthetic and photo-active proteins

Stahl, A.D.

2011

document version
Publisher's PDF, also known as Version of record

Chapter 5

The role of PufX in photochemical charge separation in the reaction centre from Rhodobacter sphaeroides: An femtosecond midIR pump-probe investigation

---

Andreas D. Stahl, Lucy I. Crouch, Michael R. Jones, Ivo van Stokkum, Rienk van Grondelle and Marie Louise Groot
Submitted to the *Journal of Pyhsical Chemistry B*

5.1 Abstract

Photochemical charge separation in isolated reaction center-light harvesting 1 (RC-LH1) complexes from Rhodobacter sphaeroides was examined using time-resolved mid-infrared pump-probe spectroscopy. Absorption difference spectra were recorded between 1760 and 1610 cm^{-1} with sub-picosecond time resolution to characterize excited state and radical pair dynamics in these complexes, via the induced absorption changes in the keto carbonyl modes of the bacteriochlorophylls and bacteriopheophytins. Experiments on RC-LH1 complexes with and without the polypeptide PufX show that its presence is required to achieve generation of the radical pair $P^+Q_A^-$ under mildly-reducing conditions. In the presence of PufX the final radical pair formed over a ∼3 ns period was $P^+Q_A^-$, but in its absence the corresponding radical pair was $P^+H_A^-$, implying that Q_A was either absent in these PufX-deficient complexes or was pre-reduced. However, $P^+Q_A^-$ could be generated in PufX-deficient complexes following addition of the oxidant DMSO, showing that Q_A was present in these complexes and allowing the conclusion that under mildly-reducing conditions charge separation was blocked after $P^+H_A^-$ due to the presence of an electron on Q_A. The data provide strong support for the hypothesis that one of the functions of PufX is to regulate the stability of Q_B^-, ensuring the oxidation of Q_A^- in the presence of a reduced quinone pool and so preserving efficient photochemical charge separation under anaerobic conditions.

5.2 Introduction

Much of our understanding of the molecular mechanism of photosynthetic energy transduction has come from studies of the structure and spectroscopic properties of the purple bacterial reaction centre (RC),

and in particular the complex from the species *Rhodobacter (Rba.) sphaeroides* (1–10). The bulk of this work has involved analysis of detergent-solubilised and purified *Rba. sphaeroides* RCs, with less emphasis on the "inner workings" of the RC when part of more intact systems. A combination of structural biology, ultrafast spectroscopy and steady-state spectroscopy has revealed that the RC uses the energy of absorbed photons to power a picosecond-timescale, three-step, membrane-spanning charge separation involving a dimer of bacteriochlorophyll (BChl) as the primary electron donor (denoted P), and a monomeric BChl (B_A), a bacteriopheophytin (H_A) and a tightly-bound ubiquinone-10 (Q_A) as sequential electron acceptors (Figure 5.1B) (1–10). The first singlet excited state of the P dimer (denoted P*) decays to form the $P^+B_A^-$ radical pair with a lifetime of 3-5 ps, with a second step of electron transfer to form $P^+H_A^-$ in <1 ps. The $P^+H_A^-$ radical pair has a lifetime of ∼200 ps, decaying principally to form $P^+Q_A^-$ (Fig 5.1B). Q_A passes two electrons, sequentially, to a second dissociable ubiquinone at the Q_B site generating, with the uptake of two protons, dihydroquinone (ubiquinol) (11, 12). In the intact *Rba. sphaeroides* cell the photo-oxidised P dimer is reduced by a water-soluble cytochrome (cyt) c_2 (13, 14), and the products of RC turnover, ubiquinol and oxidised cyt c_2, act as substrates for the protonmotive cyt bc_1 complex.

A detailed picture of the mechanism of the membrane-spanning charge separation internal to the RC has been built up through the extensive application of ultrafast visible/near-infrared (IR) transient absorbance spectroscopy (reviewed in (4–9)) and, to a lesser extent, ultrafast mid-IR transient absorbance spectroscopy (15–22). However the RC is only part of the sunlight transduction system in photosynthetic organisms. In all known purple photosynthetic bacteria the RC is associated with a light harvesting 1 (LH1) pigment-protein, forming the so-called RC-LH1 complex (23–27). The precise composition of this complex varies from species to species, but in general terms the

LH1 forms a hollow cylinder of membrane-spanning α-helices and associated BChl and carotenoid cofactors that surrounds a central RC (23–27). In some species this cylinder appears to be complete, with $\sim$32 LH1 BChls forming a ring that feeds the RC with excited state energy, whilst in other species, including *Rba. sphaeroides*, the cylinder is incomplete, with 24-30 LH1 BChls forming an arc around the central RC (Figure 5.1A, left) (see (28–30) for reviews). In *Rhodobacter* species the RC-LH1 complex is also known to contain a polypeptide termed PufX that has a single membrane-spanning α-helix and which has a strong influence on the structure of the RC-LH1 complex (see (31) for a detailed review).

In *Rba. sphaeroides* the RC-LH1 complex assembles in a dimeric form in which two RCs are surrounded and connected by an S-shaped LH1 antenna (32–38) and a monomeric form is also observed where the RC is surrounded by an open C-shaped antenna (32)(Figure 5.1A). When PufX is removed from *Rba. sphaeroides* through a gene deletion the dimeric RC-LH1 complex is no longer assembled and the monomeric complex has a larger, intact ring of LH1 pigment protein surrounding the RC (Fig. 5.1A) (38, 39). Removal of PufX also leads to a loss of capacity for photosynthetic growth, for reasons that are not fully understood (see (31) for a review of the original literature).

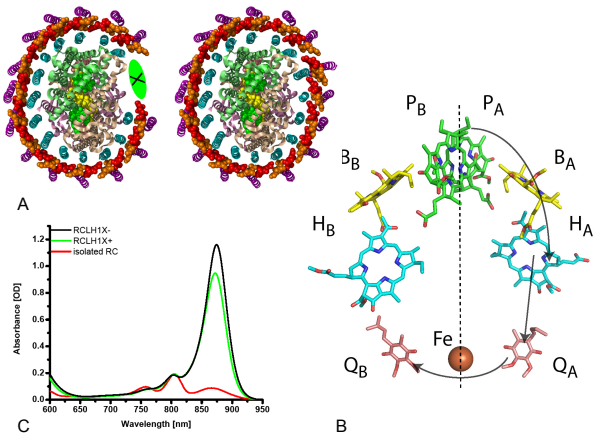

Figure 5.1: A: Periplasmic views of schematics of the PufX-containing (left) and PufX-deficient (right) RC-LH1 complexes used in this work, based on modifications of a 4.8 Å X-ray crystal structure of the RC-LH1 complex from *Rhodopseudomonas palustris* (26). The central RC (green, beige and pink ribbons) is surrounded by an LH1 antenna pigment-protein comprising an inner ring of α-polypeptides (cyan ribbons) and an outer ring of β-polypeptides (magenta ribbons), each of which has a single membrane-spanning α-helix. Between these concentric LH1 protein cylinders is a ring of BChls (shown as spheres alternating red/orange) that absorb at 875 nm. In native *Rba. sphaeroides* PufX occupies the approximate position shown by the green ellipse and interrupts the continuity of the LH1 ring (left). In the absence of PufX this ring is complete due to the presence of additional LH1 pigment-protein (right). B: Arrangement of the pigments in the reaction center of *Rhodobacter sphaeroides*. The BChl, BPhe and ubiquinone cofactors form two membrane-spanning branches, denoted A and B. The dotted line shows the axis of twofold symmetry, arrows indicate the pathway of electron transfer. The picture was created using the PDB entry 3I4D C: Absorption spectra of isolated RC (red), RC-LHI-X+ (green) and RC-LH1-X- (black) complexes.

In the present work ultrafast mid-IR spectroscopy was used to probe the characteristics of charge separation in isolated PufX-containing and PufX-deficient monomeric RC-LH1 complexes, comparing the difference spectra obtained with those from isolated RCs. To our knowledge this is the first application of ultrafast spectroscopy to R*ba. sphaeroides* RC-LH1 complexes that have been removed from the photosynthetic membrane. Although it is well known that interrogation of charge separation by ultrafast spectroscopy is complicated by the presence of an excess of antenna pigments, it has recently been shown that states functionally equivalent to the $P^+H_A^-$ and $P^+Q_A^-$ radical pairs described above can be resolved in Photosystem II core complexes (40, 41) and in intact Photosystem I complexes (42) through the application of ultrafast mid-IR spectroscopy. In addition to examining whether the LH1 pigment-protein environment modulates the characteristics of charge separation in the RC, we provide evidence for a proposed mechanistic basis of the loss of photosynthetic competence that accompanies removal of PufX from the *Rba. sphaeroides* RC-LH1 complex.

5.3 Material and Methods

5.3.1 Biological material

All *Rba. sphaeroides* strains were grown under dark/semi-aerobic conditions using M22+ medium (43) supplemented with neomycin and tetracycline (44). Starter cultures comprising 10 ml of M22+ medium in a 30 ml universal bottle were inoculated with cells taken from a glycerol stock and grown for 24 hours at 34 °C and 180 rpm in a darkened orbital incubator. Each of these were then used to inoculate 70 ml of M22+ medium in a 100 ml conical flask, and after further growth for 24 hours this intermediate culture was used to inoculate 1.5 L of M22+

medium in a 2 L conical flask. These large volume cultures were incubated for 36 hours, harvested by centrifugation and intracytoplasmic membranes prepared by cell lysis in a French pressure cell followed by ultracentrifugation, as described previously (44, 45). *Rba. sphaeroides* RCs were prepared from an antenna-deficient strain (45) as described in detail elsewhere (46). Purified RCs were stored as a concentrated solution in 20 mM Tris/HCl (pH 8.0)/0.1% lauryldimethylamine oxide (LDAO), and kept at -80 °C until used. Monomeric *Rba. sphaeroides* RC-LH1-X+ complexes were prepared from a strain lacking the LH2 antenna complex, and RC-LH1-X- complexes were prepared from a strain lacking LH2 and the PufX protein (47). Both types of complex were isolated from intracytoplasmic membranes using 4% β-dodecyl maltoside (β-DDM) (36, 48), purified by ultracentrifugation on a 5-step 20-25% (w/v) sucrose density gradient (48), and stored as a concentrated solution in 20 mM HEPES (pH 8.0)/ 0.04% DDM at -80 °C until used.

5.3.2 Sample preparation

For vis/mid-IR experiments, the sample was concentrated to an absorbance of 0.2 at 800 nm for a 20 µm optical path length. Purified RCs were suspended in 20 mM Tris-buffer in D_2O (pD 7.6) containing 0.1% LDAO, 25 µM phenazine methosulphate (PMS) and 5 mM sodium ascorbate. In case of RC-LH1 complexes two different buffers were used. The first consisted of 20 mM HEPES buffer in D_2O (pD 7.6) with 0.04% ß-DDM, 25 μM PMS and 5 mM sodium ascorbate. The other contained 20 mM HEPES buffer in D_2O (pD 7.6) with 0.04% ß-DDM and 20 mM dimethylsulfoxide (DMSO).

5.3.3 Pump-probe spectroscopy

The experimental setup consisted of an integrated Ti:sapphire oscillator-regenerative amplifier laser system (Hurricane, SpectraPhysics) operating at 1 kHz and 800 nm, producing 85 fs pulses of 0.8 mJ (49). A portion of the 800 nm light was used as pump pulse with a pulse energy of 100 nJ. The excitation pulses were focused on the sample with a 20 cm lens. A second part of the 800 nm light was used to pump an optical parametric generator and amplifier with a difference frequency generator (TOPAS, Light Conversion) to produce the mid-IR probe pulses, which were focused on the sample with a 6 cm lens. The probe and pump pulses were spatially overlapped in the sample, and after passing the sample the probe pulses were dispersed in a spectrograph (resolution 6 cm^{-1}), imaged on a 32-element MCT detector and fed into 32 home-built integrate and hold devices that were read out every shot with a National Instruments acquisition card. To ensure a fresh spot for each laser shot the sample was moved by a home-built Lissajous scanner. The polarization of the excitation pulse was set to the magic angle (54.7°) with respect to the IR probe pulses, and a phase-locked chopper operating at 500 Hz was used to ensure that the sample was excited only on every other shot such that the change in transmission could be measured. The instrument response function was about 120 fs, and all measurements were performed at room temperature.

5.3.4 Data analysis

For each excitation wavelength, a set of 100 scans for all 32 channels was averaged and 69 time points per scan were taken. Each time point was the average value of 500 laser pulses. All the collected data points were subjected to global analysis using a sequential model with increasing lifetimes (50).

5.4 Results

5.4.1 Absorbance spectra and experimental conditions

This study compared charge separation in isolated *Rba. sphaeroides* RCs with that in isolated monomeric PufX-containing RC-LH1 complexes (denoted RC-LH1-X+) and isolated monomeric PufX-deficient RC-LH1 complexes (denoted RC-LH1-X-). The complexes were isolated from intracytoplasmic membranes prepared from cells grown under semiaerobic conditions in the dark, as described in Materials and methods.

Figure 5.1C shows the Q_y absorbance spectra of the three complexes, normalized to the same absorbance at ∼802 nm. In this spectral region the LH1 antenna has a single band with a maximum at ∼870 nm, whereas the RC has three bands with maxima at 756 nm arising from the bacteriopheophytins, 802 nm arising mainly from the monomeric BChls and 867 nm arising from the primary donor BChl pair. In the RC-LH1 complexes the absorbance of LH1 at 870 nm dominates the spectrum, the 802 and 756 nm bands of the RC appear as minor components, and the 867 nm band of the RC is obscured. In PufX-deficient RC-LH1 complexes the ratio of LH1 absorbance to RC absorbance was increased due to the presence of additional BChls, in line with expectations (see above).

In this near-infrared spectral region between 650 and 950 nm absorbance changes occurring on an ultrafast time scale are dominated by the LH1 component (see Figure 5.7 of the supporting information) and the $P^+H_A^-$ and $P^+Q_A^-$ radical pairs do not have readily distinguished absorbance difference spectra. Therefore we examined a section of the mid-infrared region where it is known from FTIR difference spectroscopy (51) and recent ultrafast absorbance difference spectroscopy (20) that the H_A/H_A^- and Q_A/Q_A^- transitions give rise to distinctive

signatures of positive and negative bands. To probe function, RC and RC-LH1 complexes were excited at 800 nm, and the induced absorption changes were probed in the mid-infrared spectral region between 1730/1760 and 1610 cm^{-1} from –15 ps to 3 ns. The particular focus was to characterize the difference spectrum of the final radical pair achieved in the different complexes during the 3 ns measuring period. The collected time traces were subjected to a global analysis using a sequential scheme with increasing lifetimes in order to visualize the dynamics occurring in the system after excitation. In the limited number of previous studies of excitation trapping in *Rba. sphaeroides* RC-LH1 complexes (59–63) sodium ascorbate and/or phenazine methosulphate (PMS) were added to prevent photoaccumulation of RCs in the P^+ state (see Discussion). Accordingly, initial measurements were made in a buffer supplemented with 25 μM PMS and 5 mM sodium ascorbate to provide comparable conditions (see Materials and methods).

5.4.2 Ultrafast mid-infrared spectroscopy of RCs

In the case of the RC three components were necessary to obtain a satisfactory fit of the experimental data, with lifetimes of 4.1 ps, 250 ps and >3 ns (infinite). The evolution associated difference spectra (EADS) of these components are shown in Figure 5.2. The first EADS (Figure 5.2, solid) was typical for a BChl excited state difference spectrum in which the keto carbonyl mode, at ∼1685 cm^{-1} downshifts to 1668 cm^{-1} in the excited state, and was therefore consistent with P* (see (4) for a detailed account).

This initial component decayed with a lifetime of 4.1 ps into a second component, the EADS of which (Fig. 5.2, dashed) displayed positive bands at 1702 cm^{-1} and 1712 cm^{-1}, together with a negative band centered at 1687 cm^{-1}. The latter can be assigned to an unresolved mixture of the 9-keto modes of P_A and P_B in the ground state, which have been resolved by FTIR at 1683 cm^{-1} and 1692 cm^{-1},,

whereas the 1702 cm^{-1} and 1712 cm^{-1} bands are due to the keto carbonyls of P_A and P_B in the cation state (52–54). As discussed in detail previously (4) the lineshape of this second EADS was consistent with the radical pair $P^+H_A^-$. The bacteriopheophytin contribution in this EADS was the weak negative shoulder at 1675 cm^{-1} which has been ascribed to the 9-keto carbonyl of H_A in the neutral state, being hydrogen bonded to Glu L104 (55). Upon charge separation this mode undergoes a very strong downshift to 1591 cm^{-1} (56) accounting for the strongly positive signal appearing at the lower edge of the spectral window. The 1656 cm^{-1} negative band in the $P^+H_A^-$ spectrum has been assigned to an amide response, resulting from either an upshift to 1662 cm^{-1} in response to the formation of $P^+H_A^-$ (18, 19, 56, 57), or, in an alternative interpretation, from a downshift to 1648 cm^{-1} (54, 55). The second EADS decayed with a lifetime of 250 ps into the final EADS (Fig. 5.2, dotted) which showed a number of distinctive changes associated with the transition of $P^+H_A^-$ into $P^+Q_A^-$, including the recovery of the bleaching at 1675 cm^{-1} and the appearance of a 1667(-)/1656(+) cm^{-1} bandshift, ascribed to a protein amide I response to the charge on Q_A (18). The 1647(-)/1640(+) signal has been attributed to the response of a protein backbone C=O that is connected to Q_A via an H-bond that is perturbed upon reduction of Q_A (54, 56, 58).

The features of these three EADS recorded for RCs in the presence of sodium and ascorbate and PMS were fully consistent with previous data on mid-IR spectroscopy of *Rba. sphaeroides* RCs in the absence of reductant (15, 16, 18–20). Although EADS reflect the spectral evoloution of the system rather than representing pure states, the fact that each step of charge separation in the RC is slower than the last means that the three EADS can be attributed to P* (4.1 ps), $P^+H_A^-$ (250 ps) and $P^+Q_A^-$ (infinite). Of particular relevance to the present report are the spectral signatures of Q_A/Q_A^- and H_A/H_A^-, discussed above, and in more detail in (20). The infrared differ-

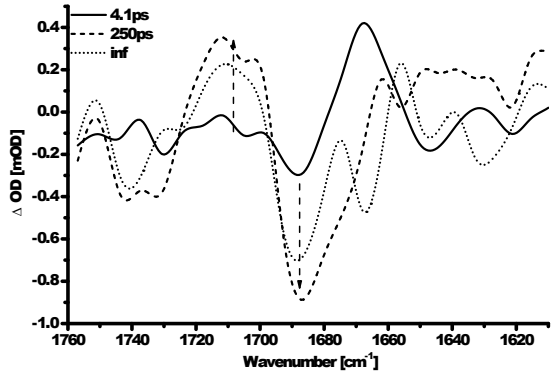

Figure 5.2: EADS obtained from the RC of *Rba. sphaeroides* after 800 nm excitation, using a global analysis with increasing lifetimes of 4.1 ps (solid to dashed spectrum), 250 ps (dashed to dotted spectrum) and an infinite (=long lived) component (dotted line).

ence spectrum of Q_A/Q_A^- shows the sequence 1667(-)/1656(+)/1647(-)/1640(+), whereas the infrared difference spectrum of H_A/H_A^- shows the sequence 1662(+)/1656(-)/1648(+). Particulary marked is the inversion between 1662(+)/1656(-) for H_A/H_A^- and 1667(-)/1656(+) for Q_A/Q_A^-.

5.4.3 Ultrafast mid-infrared spectroscopy of RC-LH1-X+ complexes

In Figure 5.3 representative time traces for the RC-LH1-X- complex in both buffer solutions used, and the RC-LH1-X+ are shown. Here it can be observed that the RC-LH1-X- complex with asc/PMS buffer (Fig. 5.3B) decays not like the other two samples (Fig. 5.3A and C), which yield a plateau reached after several hundred ps whereas this sample constantly decays over the whole timescale of acquisition. In

case of the monomeric RC-LH1-X+ complex in PMS/ascorbate buffer a set of three components was necessary to fit the spectral evolution, with lifetimes of 1.3 ps, 130 ps and >3 ns (infinite). The initial EADS was dominated by a negative band at 1648 cm^{-1} and a positive band at 1632 cm^{-1} (Figure 5.4A, solid). In addition, the spectrum displayed a small positive band at 1680 cm^{-1}, a negative band at ∼1670 cm^{-1} and a positive band at 1617 cm^{-1}. This initial component decayed in 1.3 ps into a second component (Figure 5.4A, dashed) with an EADS that showed some changes in lineshape, most notably a switch from positive to negative at 1680 cm^{-1} and an approximately 40% decrease in amplitude of the positive band at ∼1632 cm^{-1}, together with a small (∼2 cm^{-1} upshift). In contrast the bleach at 1648 cm^{-1} only slightly decreased and somewhat upshifted (∼1 cm^{-1}). The EADS of the infinite component (Figure 5.4A, dotted), formed in 130 ps, showed a further development of the positive band at 1705 cm^{-1}, the negative bands at 1680 and 1665 cm^{-1} and a further decrease of the 1648(-)/ 1635(+) cm^{-1} feature.

Previous studies of excitation transfer and trapping in RC-LH1 complexes have established that transfer of energy to the RC occurs over 30-70 picoseconds (59–64). As a result, over a 3 ns measuring window the final state formed in both RC-LH1 and RC complexes is expected to be mainly $P^+Q_A^-$, as this state is formed in ∼200 ps in isolated RCs and does not decay on the nanosecond time-scale. A caveat is that the presence of the antenna could allow for a small amount of detrapping, or long-lived antenna excited states in any LH1 complexes that are detached from RCs, and so the final difference spectrum of RC-LH1 complexes might be a composite of spectra of $P^+Q_A^-$ and LH1*. Figure 5.4C compares the EADS with an infinite lifetime for RCs (dashed) and RC-LH1-X+ complexes (solid). As can be seen the sequence 1666(-)/1655(+) cm^{-1} characteristic for Q_A/Q_A^- in the spectrum of the RC (see above) was also present in the final spectrum of the RC-LH1-X+ complex (highlighted by the vertical lines

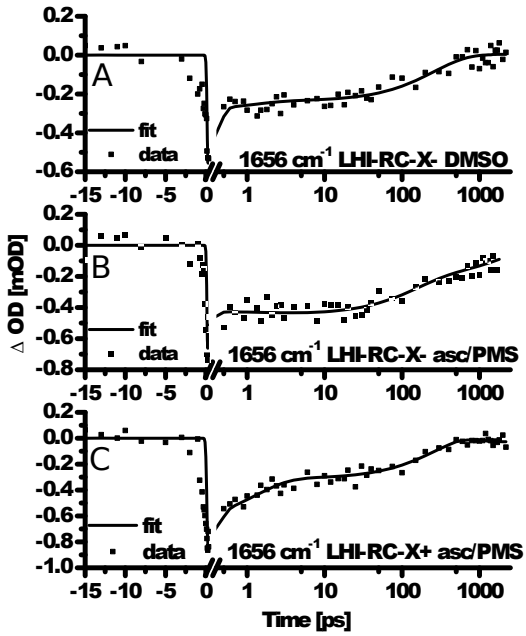

Figure 5.3: Representative time traces (scattered points) recorded at 1656 cm^{-1} for LHI-RC-X- and LHI-RC-X+ complexes in ascorbate/PMS buffer and LHI-RC-X- complexes in DMSO, and the fit through the data (solid line). The time axis is linear before t=0 and logarithmic after.

in Figure 5.4C). The 1655(+) cm^{-1} component was less pronounced in case of the RC-LH1 complex, appearing as a shoulder rather than a full band; this was probably due to the presence of LH1* contributions in this spectrum, signaled by the strong positive band at 1635 cm^{-1}. This should be accompanied by a negative LH1* band 1649 cm^{-1}

which would overlap and partially cancel out a positive Q_A^- band at 1655 cm^{-1}.

5.4.4 Ultrafast mid-infrared spectroscopy of RC-LH1-X- complexes

Time-resolved spectra for the RC-LH1-X- complex were also recorded (Figure 5.4B) to determine whether the EADS for this complex differ substantially from those of the RC-LH1-X+ complex. A set of four components were required to fit the data with lifetimes of 2.3 ps, 140 ps, 800 ps and an infinite component. The initial EADS (Figure 5.4B, solid) was very similar to that of the RC-LH1-X+ complex, with a main differential feature at 1648(-)/1632(+) cm^{-1} and a positive band at 1622 cm^{-1}. This decayed in 2.3 ps to a second EADS (Figure 5.4B, dashed) that was also very similar to the second EADS obtained for RC-LH1-X+ complexes, with a decrease in amplitude of the positive bands at 1632 and 1622 cm^{-1}. The second component decayed in 140 ps to a third component, the EADS of which (Figure 5.4B, dotted) had a much smaller differential signal at 1649(-)/1633(+) cm^{-1} of only $\sim$10% of the initial amplitude, a pronounced positive band at 1711 cm^{-1}, and negative bands at 1679 and 1649 cm^{-1} , respectively. The EADS of the final state (Figure 5.4B, dash-dotted) had a relatively low amplitude compared to its predecessors. Thus, although the first two components required to fit the data for the RC-LH1-X+ and RC-LH1-X- complexes were similar in terms of line shape and amplitude, being dominated by spectral features indicative of LH1*, the subsequent components showed differences between the two sets of data.

Comparison of the final EADS for the RC-LH1-X+ and RC-LH1-X- complexes revealed that the characteristics of Q_A/Q_A^- seen in the spectrum of the RC-LH1-X+ complex (Figure 5.4D, solid), namely the sequence 1664(-)/1655(+), was absent in the spectrum of the RC-LH1-

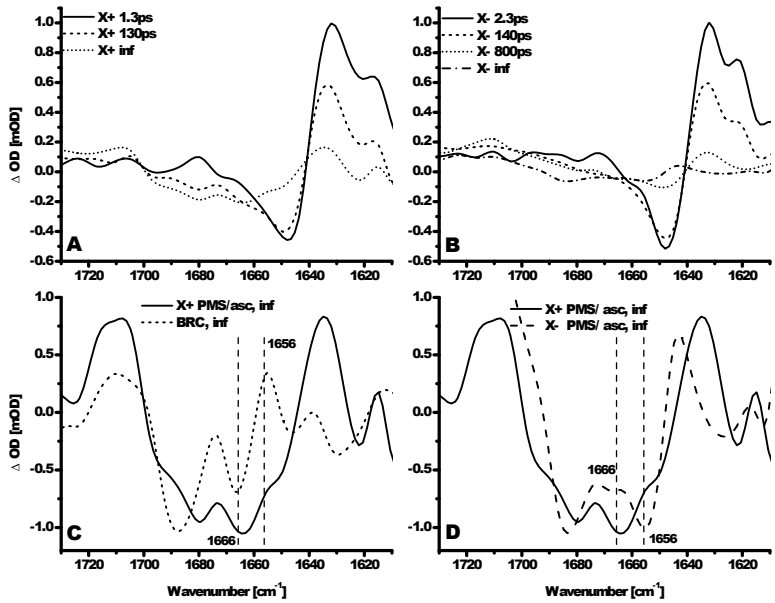

Figure 5.4: EADS for RC-LH1 complexes in ascorbate/PMS. (A): EADS obtained for RC-LH1-X+ complexes using a global analysis with increasing lifetimes of 1.3 ps, 130 ps and a inifinite component. (B) EADS obtained for RC-LH1-X- complexes using a global analysis with increasing lifetimes of 2.3 ps, 140 ps and an infinite component. (C) Comparison of final EADS for RC and RC-LH1-X+ complexes with marker bands typical for a $P^+Q_A^-$ state at 1656 and 1666 cm^{-1} highlighted. (D) Comparison of EADS for RC-LH1-X+ and RC-LH1-X- complexes with marker band inversion at 1656 and 1666 cm^{-1} highlighted

X- complex (Figure 5.4D, dashed). Instead this had a positive band at 1665 cm^{-1}, a negative band at 1655 cm^{-1} and a positive band at 1643 cm^{-1}, a pattern characteristic of a H_A/H_A^- difference spectrum (see above). To emphasize this finding, in Figure 5.5A the final EADS for the RC-LH1-X- complex (dashed) is compared with the $PH_A/P^+H_A^-$ difference spectrum from FTIR spectroscopy (65) (solid) and the 250 ps ($P^+H_A^-$) EADS of the RC from the present work (dotted). All three spectra have the distinct signature 1663(+)/1656(-)/1644(+) in common (within +- 2 cm^{-1}), a signature quite distinct from the 1667(-)/1656(+)/1647(-) pattern expected for the state $P^+Q_A^-$. This strongly indicated that the final state achieved in the RC-LH1-X- complex in the presence of mild reductant was $P^+H_A^-$ rather than $P^+Q_A^-$ seen in the RC and RC-LH1-X+ complexes under the same conditions.

Possible implications of charge separation being halted at the radical pair $P^+H_A^-$ in the RC-LH1-X- complex are that Q_A is either already reduced, or is absent. To our knowledge the properties of a PufX-deficient RC-LH1 complex have not been studied previously by ultrafast spectroscopy, but some study has been made of interactions between RC-LH1-X- complexes and the cytochrome bc_1 complex through millisecond time-scale spectroscopy by Comayras and co-workers (66, 67). In that study (and others) there was no indication that RC-LH1-X- complexes assemble without a Q_A quinone. Rather, it was concluded that in membranes with PufX-deficient RC-LH1 complexes, reduction of the quinone pool leads to a larger degree of reduction of Q_A than is the case for membranes with RC-LH1-X+ complexes (70% Q_A^- with an 80% reduced pool vs 20% Q_A^- for RC-LH1-X+ complexes under the same condtions) (66, 67). The likely explanation of the data summarized in Figure 5.5A is therefore that under the experimental conditions charge separation in RC-LH1-X+ complexes produces (mainly) $P^+Q_A^-$ but in RC-LH1-X- complexes produces (mainly) $P^+H_A^-$ because of the presence of Q_A [U+2011]. This is in agreement with a low yield of $P^+H_A^-$ on the long time scale in the

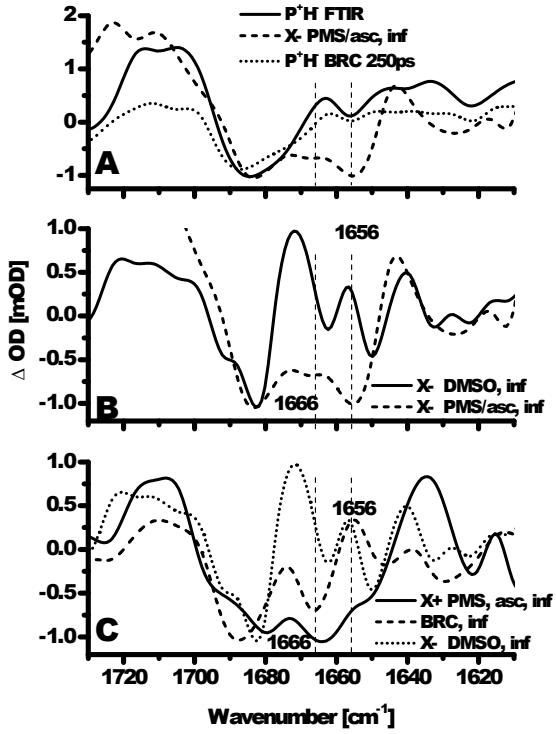

Figure 5.5: Influence of experimental conditions on the final readical pair formed in RC-LH1-X- complexes. (A) Comparison of chemically generated FTIR spectrum of P^+H^- in RCs with the final EADS for RC-LH1-X- complexes in ascorbate/PMS and the RC EADS with a 250 ps lifetime attributed to $P^+H_A^-$ state. (B) Comparison of the final EADS for RC-LH1-X- complexes in ascorbate/PMS and DMSO. Marker bands for $P^+H_A^-$ and $P^+Q_A^-$ at 1656 and 1666 cm-1 are indicated. (C) Comparison of final EADS of RC-LH1-X+ and RC complexes in ascorbate/PMS and RC-LH1-X- complexes in DMSO.

RC-LH1-X- complexes, as in the presence of Q_A^- the state $P^+H_A^-$ recom-

bines with a lifetime of several nanoseconds in isolated RCs (68, 69).

The current observations add weight to an explanation put forward by Comayras and co-workers to account for the fact that RC-LH1-X- complexes cannot support photosynthetic growth of *Rba. sphaeroides* under illuminated/anaerobic conditions in standard growth media. Such conditions are expected to produce a reduced quinone pool which would lead to larger than normal reduction of Q_A and a loss of charge separation in RC-LH1-X- complexes compared with native RC-LH1-X+ complexes (see Discussion, below). In support of this, it has been found that photosynthetic growth can be restored to PufX-deficient strains of *Rba. sphaeroides* by supplementing the medium with the oxidant dimethylsulphoxide (DMSO) (70–72) the explanation being that DMSO drains electrons from the quinone pool, oxidizing Q_A and restoring charge separation and light-driven cyclic electron transfer. This observation raises the question of whether the final state observed in RC-LH1-X- complexes would be different in buffer supplemented with DMSO rather than ascorbate/PMS.

To test this, energy transfer, trapping and charge separation were examined by ultrafast spectroscopy of RC-LH1-X- complexes suspended in 20 mM HEPES/D_2O (pD 7.6)/0.04% β-DDM/20 mM DMSO. In this case a set of three components were required to fit the data, with lifetimes of 1.7 ps, 270 ps and >3 ns (infinite). Figure 5.6A compares the EADS for the first component for RC-LH1-X+ and RC-LH1-X- complexes in ascorbate/PMS (solid and dotted, respectively) and RC-LH1-X- complexes in DMSO (dashed). The spectra of the RC-LH1-X- and RC-LH1-X+ complexes in ascorbate/PMS resembled each other very well, especially in the 1650 to 1630 cm^{-1} region and the associated lifetimes were similar (1.3 ps vs. 2.3 ps). The initial EADS of the RC-LH1-X- complex in DMSO (lifetime 1.7 ps) had the same general lineshape, but the dominant differential signal was shifted $\sim$11 cm^{-1} towards lower wavenumbers. In addition the bleach around 1640 cm^{-1} was somewhat narrower than for the equivalent two spectra, with a

shoulder at 1645 cm^{-1}.

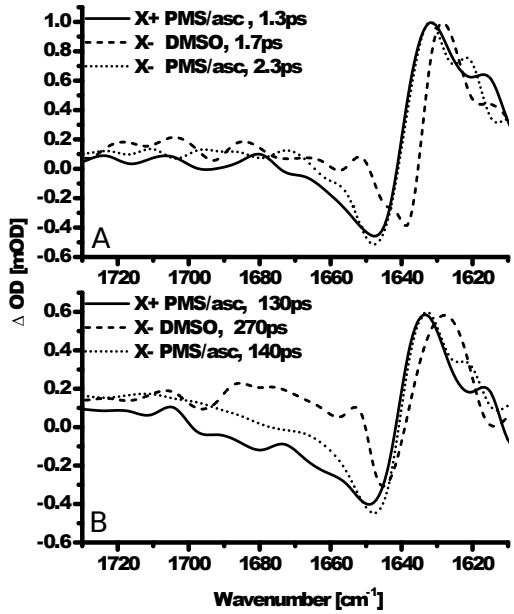

Figure 5.6: EADS for RC-LH1 complexes in ascorbate/PMS. or DMSO. Comparison of the (A) first and (B) second EADS obtained using a global analysis with increasing lifetimes for RC-LH1-X+ and RC-LH1X- in PMS/ascorbate and RC-LH1-X- complexes in DMSO.

Fig. 5.6B compares EADS of the next component; again, correspondence between the spectra for the two complexes in ascorbate/PMS was high. The main variation for the second EADS of the RC-LH1-X- complex in DMSO was qualitatively the same as for the spectra of the initial component, with the main differential signal downshifted to lower wavenumbers and a narrowing of the ground state band at

1645 cm^{-1}. The associated lifetime of this component for RC-LH1-X- complexes in DMSO was 270 ps, twice as long as the 130 and 140 ps seen for both types of complex in ascorbate/PMS, but closer to the 250 ps seen for the second component in isolated RCs in ascorbate/PMS and 222/280 ps for the same component in the absence of ascorbate/PMS (20). A comparison of the EADS of the final components for RC-LH1-X- complexes in DMSO and ascorbate/PMS is presented in Figure 5.5B. Clear differences at ∼1666 cm^{-1} and ∼1656 cm^{-1} could be observed, with the signature 1665(+)/1656(-) in ascorbate/PMS changing to 1662(-)/1657(+) in DMSO, suggesting that addition of the oxidant had changed the final radical pair from $P^+H_A^-$ to $P^+Q_A^-$. To emphasise this, in Figure 5.5C the final EADS for RCs in ascorbate/PMS (dashed), RC-LH1-X+ complexes in ascorbate/PMS (solid) and RC-LH1-X- complexes in DMSO (dotted) are overlaid. In all three spectra the 1666(-)/1656(+) cm^{-1} fingerprint of the $P^+Q_A^-$ radical pair was found (whin an accuracy of +- 2 cm^{-1}), in marked contrast to the case of RC-LH1-X- complexes in ascorbate/PMS where charge separation was limited to $P^+H_A^-$.

5.5 Discussion

The initial aim of the work described in this report was to investigate charge separation in *Rba. sphaeroides* RCs in the presence of the accompanying LH1 antenna protein. The kinetics and mechanism of this process have been studied extensively in purified RCs and in RCs in antenna-deficient membranes, but there have been only a very few studies of picosecond time-scale events in intact RC-LH1 complexes, and these have been limited to investigation of excitation trapping in membrane-bound complexes, employing mutants that lack the peripheral LH2 antenna (59–63, 73). To our knowledge the present work is the first attempt to examine the dynamics of energy transfer and

charge separation in a purified RC-LH1 complex.

A technical issue when examining the properties of the RC-LH1 complex by laser spectroscopy is the problem of photogenerating a long-lived P^+ state that "closes" the RC. This issue is less problematic in the case of purified RC because charge separation will lead to the formation of $P^+Q_A^-$ or $P^+Q_B^-$ that have lifetimes of 100 ms or 1 s, respectively ($P^+Q_A^-$ being formed in RCs where the Q_B quinone has been lost during purification). As a result it is relatively straightforward to ensure that purified RCs are fully relaxed to the PQ_AQ_B ground state by combining a suitable rate of excitation pulses with movement of the sample and, perhaps, inhibition of $Q_AQ_B^-$ formation. However, in more intact systems there is the possibility of translocated electrons being lost to the ubiquinone pool, leaving a very long-lived P^+ state if the natural reductant (cyt c_2) is absent. To avoid this situation previous studies of membrane-bound RC-LH1 complexes have employed addition of sodium ascorbate and/or PMS to ensure slow reduction of P^+ between excitations (59–63, 73). In the present study RC-LH1 complexes were removed from the membrane and purified on sucrose density gradients, but it is known that such complexes are associated with a mini-pool of up to 15 ubiquinones, and the lifetime of the $P^+Q_B^-$ state is of the order of three to five-fold longer than in purified RCs (66, 67, 74, 75). As a result ultrafast mid-infrared spectroscopy was carried out in the presence of sodium ascorbate and PMS to be consistent with previous work. These reagents have mid-point redox potentials (Em) of around 40 mV and 50 mV, respectively, at pH 8.0 (76), which makes them suitable for reduction of P^+ (Em $\sim$ 450-500 mV depending on presence of membrane and antenna (77)). However they should not directly reduce Q_A which has an Em of -45 mV in isolated RCs (78) and -80 mV in photosynthetic membranes at pH 8.0 (79).

Ultrafast spectroscopy was first applied to RCs. EADS and associated lifetimes (4.1 ps, 250 ps and infinite) obtained for purified RCs

in the presence of ascorbate/PMS (with 800 nm excitation) showed good correspondence to those determined in a previous study (3.6 ps, 280 ps and infinite) obtained in the absence of ascorbate/PMS (with 860 nm excitation) (20). This showed that the presence of the mild reductant and mediator did not have a significant influence on the kinetics of primary or secondary charge separation, or on the lineshapes of the EADS attributed to the P*, $P^+H_A^-$ and $P^+Q_A^-$ states formed. The dominant feature of the first and second EADS obtained for both types RC-LH1 complex in ascorbate/PMS was a strong differential signal with a negative band corresponding to the ground state mode being at around 1648 cm^{-1} and a positive band corresponding to the downshifted excited state mode at around 1632 cm^{-1}. We attribute this feature to a downshift of the keto carbonyl modes of the LH1 antenna BChls on formation of the LH1* excited state. The equivalent strong downshift of the keto modes of the P BChls of the RC on formation of P* gave rise to a differential signal at 1688(-)/1668(+) cm^{-1} (Figure 5.2, dotted). The size of the downshift was therefore similar in the two cases, 16 cm^{-1} and 20 cm^{-1}, respectively, but there was a strong difference ($\sim$40 cm^{-1}) in the absolute positions of the two ground state modes in purified RCs and purified RC-LH1 complexes. It should also be noted that the peak frequency of this ground state mode (1648 cm^{-1}) for the keto carbonyls of the LH1 BChls in the isolated RC-LH1-X+ and RC-LH1-X- complexes analysed in the present study was somewhat lower than the 1661 cm^{-1} reported for the keto carbonyl groups of the LH1 BChls determined by FT-Raman spectroscopy of both RC-LH1-X+ and LH1-only complexes embedded in native *Rba. sphaeroides* membranes (80, 81) and purified *Rba. sphaeroides* LH1 complexes (82).

The reasons for low frequency of the ground state mode of the LH1 keto carbonyls in the present study are not clear, but it is known that the stretching frequency of the keto carbonyl mode of chlorins and bacteriochlorins is sensitive to hydrogen bonding and the polarity of

the surroundings of the group (83). As an example, the stretching frequency of the keto carbonyl of BChl a has been reported to be at 1684 cm^{-1} in tetrahydrofuran but at 1652 cm^{-1} in hydrogen-bonding methanol (55, 84), and this stretching frequency has been reported to be as low as 1635 cm^{-1} in BChl-water micelles (85). The reason for the low stretching frequency observed for RC-LH1 complexes in the present report will require further investigation, but it is interesting to note that the position of this band further downshifted when ascorbate/PMS in the measuring buffer was replaced by 20 mM DMSO (Figure 5.6). This indicated that the stretching frequency was sensitive to the conditions of the experiment, one possibility being that these keto groups are engaged in hydrogen-bonds, and the strength of these was modulated by the conditions of the experiment (with a stronger hydrogen bond producing a lower frequency).

Although not yet explained, the strong difference in the lineshape of the P/P* EADS in Figure 5.2(solid) and initial LH1/LH1* EADS in Figure 5.6 gave the possibility of assessing the contribution of the RC to the early spectral evolution of the system. In the case of both types of RC-LH1 complex the 800 nm pump pulse achieved direct excitation of RCs as well as some excitation of the blue wing of the LH1 absorbance. Based on transient absorption in the near-IR, Xiao et al (63) concluded that excitation at 800 nm results in ∼50% direct excitation of RCs, and that the probability of detrapping of excitation energy to LH1 from P* is very low, with a rate of 8 ps^{-1}. However, the contribution of RC* in our t=0 spectra was significantly smaller than 50% and it appeared to be dominated by LH1* features, see solid lines in Figure 5.4 A and B. This may be due to the response of the keto carbonyls being stronger in LH1 than in RC, or, reflect a relatively larger population of LH1* than of RC*, under our excitation conditions.

On the timescale of 1.3 and 2.3 ps, respectively, an RC $P^+H_A^-$ contribution becomes visible, via the bleaching of the P-keto bands at

1688 cm^{-1}, representing primary charge separation between P and H_A, occurring via $P^* \rightarrow P^+B_A^- \rightarrow P^+H_A^-$, in the fraction of directly excited RCs. Note that also in the isolated RC this process is accompanied by an increase in the keto band around 1688 cm^{-1}. Concomitant a decay of LH1* signal takes place. As the current experiments were not performed under annihilation free conditions, this process may represent singlet-singlet annihilation in LH1. Attribution of the second component, with lifetimes of 130 and 140 ps, respectively, was less clear. In previous studies of energy transfer in membrane bound RC-LH1 complexes a component of ∼46 ps (59) ∼37 ps (63) or ∼72 ps (73) has been reported, and interpreted as transfer of energy from the antenna to the RC (trapping), whereas slower minor components have been attributed to secondary electron transfer from $P^+H_A^- \rightarrow P^+Q_A^-$, or recombination of P* from $P^+H_A^-$ in RCs where electron transfer to Q_A was blocked. In the present study the lifetime of the second EADS could reflect these processes, perhaps originating from different sources given the evidence from the final EADS that the step $P^+H_A^-$ $\rightarrow P^+Q_A^-$ was active in RC-LH1-X+ complexes but not in RC-LH1-X- complexes when ascorbate/PMS was present.

A marked effect of DMSO was its impact on the lifetime of the second EADS required to fit the time-resolved spectra. In the presence of ascorbate/PMS this lifetime was 130 ps for RC-LH1-X+ complexes and 140 ps for RC-LH1X- complexes, but became 270 ps when the latter were examined with DMSO in the measuring buffer. A lifetime of 270 ps is close to the value of 250 ps obtained for the lifetime of $P^+H_A^-$ in RCs in ascorbate/PMS in the present study, and lifetimes of 280 ps and 222 ps obtained for RCs without oxidant or reductant in previous work (20). Again, attribution of this lifetime and explanation of why it varies will require further experiments and modeling.

The most surprising finding in the analysis of the two types of RC-LH1 complex under mildly reducing conditions was the difference in the lineshape of the final EADS, which had a lifetime in excess

of the 3 ns time-window of the experiment. Again, bearing in mind the complex nature of the experiment with excitation of both antenna and RC at 800 nm, the lineshape of the EADS obtained for the RC-LH1-X+ complex was consistent with that expected for $P^+Q_A^-$, with clear evidence of the spectral signature of the Q_A/Q_A^- transition. In contrast, the final EADS for the RC-LH1-X- complex had a lineshape consistent with $P^+H_A^-$, suggesting that Q_A was either absent from this complex or was (mainly) reduced under the particular experimental conditions. Replacement of mildly reducing ascorbate/PMS in the measuring buffer by mildly oxidizing DMSO (20 mM, Em,7.6 = 125 mV) led to a final EADS for the RC-LH1-X- complex that now had the spectral signature of Q_A/Q_A^-, showing that Q_A was not absent from this complex and that the contrasting results with ascorbate/PMS must have been due to Q_A being (mostly) oxidised in RC-LH1-X+ complexes and (mostly) reduced in RC-LH1-X- complexes.

As outlined above, this finding provides support for a hypothesis put forward by Comayras et al. in 2005 (66, 67) to explain the very strong effect of deletion of the gene encoding PufX on the capacity for growth of *Rba. sphaeroides* under standard anaerobic/illuminated heterotrophic conditions (see (31) for a detailed review). The RC-LH1 complexes that are assembled in these PufX-deficient strains have a higher-than-normal complement of LH1 BChls per RC (Figure 5.1B), and in *Rba. sphaeroides* it has been established that the LH1 antenna forms a closed cylinder of pigment-protein complex around the RC, rather than the open cylinder formed when PufX is present (38, 39). Initially it was generally thought that this closed cylinder provides a physical obstruction to the exchange of ubiquinone/ubiquinol between the RC and cytochrome bc_1 complex. However it was subsequently shown that PufX had minimal effects on such exchange under conditions where the quinone pool consisted of a mixture of ubiquinone and ubiquinol, but was important for ubiquinol release and/or diffusion to the bc_1 complex when the quinone pool was mostly oxidised,

and ubiquinone diffusion and/or binding to the RC under conditions where the pool was mostly reduced (70, 71). It was then established that there was a two to three-fold slowing of the rate of turnover of quinone at the Q_B site of RC-LH1 complexes in the absence of PufX in both membranes and isolated complexes, and the rate of diffusion of quinol from the RC to the cytochrome bc1 complex was also slowed by a factor of two (66, 67). In addition, Comayras and coworkers showed that the rate of $P^+Q_B^-$ recombination was slowed by a factor of four in RC-LH1-X- complexes, and the rate of the second electron transfer from Q_A to Q_B (i.e. the reaction $Q_A^-Q_B^- + 2H^+ \rightarrow Q_AQ_BH_2$) was slowed by a factor of six, both of which would indicated a stabilization of Q_B^- in the absence of PufX (66, 67). Given this, Comayras and coworkers proposed that the lack of photosynthetic growth seen in PufX-deficient strains is due to most RCs being in the state Q_A^- under anaerobic/illuminated growth conditions, the rationale being that when Q_B^- is stabilised the equilibrium of the above reaction will favour the $Q_A^-Q_B^-$ state. As a result, as the quinone pool and then Q_B becomes reduced under anaerobic conditions, Q_A will be more easily reduced in RC-LH1-X- complexes than in RC-LH1-X+ complexes.

An attractive feature of this hypothesis is that it explains the observation that growth of PufX-deficient strains under anaerobic, illuminated conditions can be restored by supplementing the growth medium with DMSO (70–72). Here the rationale is that electron flow to DMSO partially oxidises the ubiquinone pool, oxidizing Q_B and Q_A and opening the RC for catalysis of cyclic electron transfer despite the absence of PufX. In fact it is known that anaerobic/illuminated growth of the closely-related *Rba. capsulatus* on a strongly reducing carbon source such as butyrate or propionate is only possible if the medium is supplemented with an auxiliary oxidant such as DMSO in order to prevent over-reduction of the quinone pool and Q_A (86), and redox poising of the *Rba. capsulatus* photosynthetic electron transfer chain by DMSO has been demonstrated experimentally (87).

The findings from ultrafast mid-infrared spectroscopy in the present work strongly support the hypothesis of Comayras and co-workers that a consequence of deletion of PufX is a deleterious shift in the redox equilibrium between Q_A, Q_B and the ubiquinone pool. The marked difference in the final radical pair state achieved in RC-LH1-X+ and RC-LH1-X- complexes in the presence of ascorbate/PMS points towards Q_A being reduced in the latter but not in the former despite the identical conditions used for bacterial growth, protein purification and measurement of charge separation. It is not clear whether this difference in the redox state of Q_A was already present during cell growth, harvesting, and extraction/purification of RC-LH1 complexes, or whether it was induced by the use of ascorbate and PMS in the measuring buffer. However, it is clear that Q_A is (mostly) oxidised when charge separation is measured in RC-LH1-X- complexes in the presence of DMSO, further validating the proposals of Comayras and co-workers (66, 67) and providing a neat correlation between results of ultrafast spectroscopy and measurements of the impact of DMSO on photosynthetic growth of PufX-deficient strains (70–72). What has emerged is a specific role for PufX in regulating the redox properties of Q_B to ensure that membrane-spanning charge separation to Q_A can still take place under conditions where the intramembrane quinone pool is mainly reduced. How PufX achieves this is as yet unclear, and further experiments are being directed towards understanding this.

5.6 Conclusions

We performed time-resolved midIR absorption difference experiments on RC-LH1 complexes with and without the PufX complex. Our experiments show that the PufX complex is required to generate the state $P^+Q_A^-$, as in the absence of PufX, electron transfer is blocked after the bacteriopheophytin acceptor. Experiments forcing oxidation

of Q_A^- by DMSO, show that this is due to the presence of Q_A^-. The experiments provide therefore strong support for the hypothesis that the function of the polypeptide PufX is to oxidize Q_A^- under conditions of a partially reduced ubiquinone pool, a requirement for photosynthetic function.

Bibliography

[1] J. P. Allen, G. Feher, T. O. Yeates, H. Komiya, and D. C. Rees. Structure of the reaction center from rhodobacter-sphaeroides r-26 - the cofactors .1. *Proceedings of the National Academy of Sciences of the United States of America*, 84(16):5730–5734, 1987.

[2] C. H. Chang, O. Elkabbani, D. Tiede, J. Norris, and M. Schiffer. Structure of the membrane-bound protein photosynthetic reaction center from rhodobacter-sphaeroides. *Biochemistry*, 30(22):5352–5360, 1991.

[3] U. Ermler, G. Fritzsch, S. K. Buchanan, and H. Michel. Structure of the photosynthetic reaction-center from rhodobacter-sphaeroides at 2.65-angstrom resolution - cofactors and protein-cofactor interactions. *Structure*, 2(10):925–936, 1994.

[4] A.J. Hoff and J. Deisenhofer. Photophysics of photosynthesis: Structure and spectroscopy of reaction centres of purple bacteria. *Physics Reports-Review Section Of Physics Letters*, 287:2–247, 1997.

[5] M. R. Jones. The petite purple photosynthetic powerpack, 2009.

[6] W.W. Parson. Reaction centers. In H. Scheer, editor, *Chlorophylls*, pages 1153–1180. CRC Press, Boca Raton, 1991.

[7] W. W. Parson. Photosynthetic bacterial reaction centers. In D.S Bendall, editor, *Protein Electron Transfer*, pages 125–160. BIOS Scientific Publishers, Oxford, 1996.

[8] M.E. van Brederode and M. R. Jones. Reaction centres of purple bacteria. In N. S. Scrutton and A Holzenburg, editors, *Enzyme-Catalysed Electron and Radical Transfer*. Kluwer Academic/Plenum Publishers, New York, 2000.

[9] N. W. Woodbury and J. P. Allen. The pathway, kinetics and thermodynamics of electron transfer in wild type and mutant bacterial reaction centers of purple nonsulfur bacteria. In Madigan M.T. Blankenship, R.E. and C.E. Bauer, editors, *Anoxygenic Photosynthetic Bacteria*, pages 527–557. Kluwer Academic Publishers, 1995.

[10] W. Zinth and J. Wachtveitl. The first picoseconds in bacterial photosynthesis–ultrafast electron transfer for the efficient conversion of light energy. *Chemphyschem*, 6(5):871–80, 2005.

[11] M. Y. Okamura, M. L. Paddock, M. S. Graige, and G. Feher. Proton and electron transfer in bacterial reaction centers. *Biochimica Et Biophysica Acta-Bioenergetics*, 1458(1):148–163, 2000.

[12] C. A. Wraight. Proton and electron transfer in the acceptor quinone complex of photosynthetic reaction centers from rhodobacter sphaeroides. *Frontiers in Bioscience*, 9:309–337, 2004.

[13] H.L. Axelrod and M. Y. Okamura. The structure and function of the cytochrome c2: reaction center electron transfer complex from rhodobacter sphaeroides. *Photosynthesis Research*, 85, 2005.

[14] Taras V. Pogorelov, Felix Autenrieth, Elijah Roberts, and Zaida A. Luthey-Schulten. Cytochrome c2 exit strategy:â dissociation studies and evolutionary implications. *The Journal of Physical Chemistry B*, 111(3):618–634, 2006.

[15] P. Hamm and W. Zinth. Ultrafast initial reaction in bacterial photosynthesis revealed by femtosecond infrared-spectroscopy. *Journal of Physical Chemistry*, 99(36):13537–13544, 1995.

[16] P. Hamm, M. Zurek, W. Mantele, M. Meyer, H. Scheer, and W. Zinth. Femtosecond infrared-spectroscopy of reaction centers from rhodobacter-sphaeroides between 1000 and 1800 cm(-1). *Proceedings of the National Academy of Sciences of the United States of America*, 92(6):1826–1830, 1995.

[17] Gilad Haran, Klaas Wynne, Chris C. Moser, P. Leslie Dutton, and Robin M. Hochstrasser. Level mixing and energy redistribution in bacterial photosynthetic reaction centers. *The Journal of Physical Chemistry*, 100(13):5562–5569, 1996.

[18] S. Maiti, B. R. Cowen, R. Diller, M. Iannone, C. C. Moser, P. L. Dutton, and R. M. Hochstrasser. Picosecond infrared studies of the dynamics of the photosynthetic reaction center. *Proceedings of the National Academy of Sciences of the United States of America*, 90(11):5247–5251, 1993.

[19] S. Maiti, G. C. Walker, B. R. Cowen, R. Pippenger, C. C. Moser, P. L. Dutton, and R. M. Hochstrasser. Femtosecond coherent transient infrared-spectroscopy of reaction centers from rhodobacter-sphaeroides. *Proceedings of the National Academy of Sciences of the United States of America*, 91(22):10360–10364, 1994.

[20] N. P. Pawlowicz, R. van Grondelle, I. H. M. van Stokkum, J. Breton, M. R. Jones, and M. L. Groot. Identification of the first steps in charge separation in bacterial photosynthetic reaction centers of rhodobacter sphaeroides (vol 95, pg 1268, 2008). *Biophysical Journal*, 95(8):4089–4089, 2008.

[21] G. C. Walker, S. Maiti, B. R. Cowen, C. C. Moser, P. L. Dutton, and R. M. Hochstrasser. Time resolution of electronic transitions of photosynthetic reaction centers in the infrared. *The Journal of Physical Chemistry*, 98(22):5778–5783, 1994.

[22] Klaas Wynne, Gilad Haran, Gavin D. Reid, Chris C. Moser, P. Leslie Dutton, and Robin M. Hochstrasser. Femtosecond infrared spectroscopy of low-lying excited states in reaction centers of rhodobacter sphaeroides. *The Journal of Physical Chemistry*, 100(12):5140–5148, 1996.

[23] R. J. Cogdell, A. Gall, and J. Kohler. The architecture and function of the light-harvesting apparatus of purple bacteria: from single molecules to in vivo membranes. *Quarterly Reviews of Biophysics*, 39(3):227–324, 2006.

[24] R. J. Cogdell, A. T. Gardiner, A. W. Roszak, C. J. Law, J. Southall, and N. W. Isaacs. Rings, ellipses and horseshoes: how purple bacteria harvest solar energy. *Photosynthesis Research*, 81(3):207–214, 2004.

[25] X. C. Hu, T. Ritz, A. Damjanovic, F. Autenrieth, and K. Schulten. Photosynthetic apparatus of purple bacteria. *Quarterly Reviews of Biophysics*, 35(1):1–62, 2002.

[26] A. W. Roszak, T. D. Howard, J. Southall, A. T. Gardiner, C. J. Law, N. W. Isaacs, and R. J. Cogdell. Crystal structure of the

rc-lh1 core complex from rhodopseudomonas palustris. *Science*, 302(5652):1969–1972, 2003.

[27] S. Scheuring, D. Levy, and J. L. Rigaud. Watching the components of photosynthetic bacterial membranes and their in situ organisation by atomic force microscopy. *Biochimica Et Biophysica Acta-Biomembranes*, 1712(2):109–127, 2005.

[28] S. Scheuring. Afm studies of the supramolecular assembly of bacterial photosynthetic core-complexes. *Current Opinion in Chemical Biology*, 10(5):387–393, 2006.

[29] J. N. Sturgis and R. A. Niederman. Atomic force microscopy reveals multiple patterns of antenna organization in purple bacteria: implications for energy transduction mechanisms and membrane modeling. *Photosynthesis Research*, 95(2-3):269–278, 2008.

[30] J. N. Sturgis, J. D. Tucker, J. D. Olsen, C. N. Hunter, and R. A. Niederman. Atomic force microscopy studies of native photosynthetic membranes. *Biochemistry*, 48(17):3679–3698, 2009.

[31] K. Holden-Dye, L. I. Crouch, and M. R. Jones. Structure, function and interactions of the pufx protein. *Biochim Biophys Acta*, 1777(7-8):613–30, 2008.

[32] S. Bahatyrova, R. N. Frese, C. A. Siebert, J. D. Olsen, K. O. van der Werf, R. van Grondelle, R. A. Niederman, P. A. Bullough, C. Otto, and C. N. Hunter. The native architecture of a photosynthetic membrane. *Nature*, 430(7003):1058–1062, 2004.

[33] F. Francia, J. Wang, G. Venturoli, B. A. Melandri, W. P. Barz, and D. Oesterhelt. The reaction center-lh1 antenna complex of rhodobacter sphaeroides contains one pufx molecule

which is involved in dimerization of this complex. *Biochemistry*, 38(21):6834–6845, 1999.

[34] C. Jungas, J. L. Ranck, J. L. Rigaud, P. Joliot, and A. Vermeglio. Supramolecular organization of the photosynthetic apparatus of rhodobacter sphaeroides. *Embo Journal*, 18(3):534–542, 1999.

[35] P. Qian, P. A. Bullough, and C. N. Hunter. Three-dimensional reconstruction of a membrane-bending complex - the rc-lh1-pufx core dimer of rhodobacter sphaeroides. *Journal of Biological Chemistry*, 283(20):14002–14011, 2008.

[36] P. Qian, C. N. Hunter, and P. A. Bullough. The 8.5 angstrom projection structure of the core rc-lh1-pufx dimer of rhodobacter sphaeroides. *Journal of Molecular Biology*, 349(5):948–960, 2005.

[37] S. Scheuring, F. Francia, J. Busselez, B. A. Melandri, J. L. Rigaud, and D. Levy. Structural role of pufx in the dimerization of the photosynthetic core complex of rhodobacter sphaeroides. *Journal of Biological Chemistry*, 279(5):3620–3626, 2004.

[38] C. A. Siebert, P. Qian, D. Fotiadis, A. Engel, C. N. Hunter, and P. A. Bullough. Molecular architecture of photosynthetic membranes in rhodobacter sphaeroides: the role of pufx. *Embo Journal*, 23(4):690–700, 2004.

[39] T. Walz, S. J. Jamieson, C. M. Bowers, P. A. Bullough, and C. N. Hunter. Projection structures of three photosynthetic complexes from rhodobacter sphaeroides: Lh2 at 6 angstrom lh1 and rc-lh1 at 25 angstrom. *Journal of Molecular Biology*, 282(4):833–845, 1998.

[40] Mariangela Di Donato, Rachel O. Cohen, Bruce A. Diner, Jacques Breton, Rienk van Grondelle, and Marie Louise Groot. Primary

charge separation in the photosystem ii core from synechocystis: A comparison of femtosecond visible/midinfrared pump-probe spectra of wild-type and two p680 mutants. *Biophysical Journal*, 94(12):4783–4795, 2008.

[41] N. P. Pawlowicz, M. L. Groot, I. H. M. van Stokkum, J. Breton, and R. van Grondelle. Charge separation and energy transfer in the photosystem ii core complex studied by femtosecond midinfrared spectroscopy. *Biophysical Journal*, 93(8):2732–2742, 2007.

[42] M. Di Donato, A. D. Stahl, I. H. M. van Stokkum, R. van Grondelle, and M. L. Groot. Cofactors involved in light-driven charge separation in photosystem i identified by subpicosecond infrared spectroscopy. *Biochemistry*, 50(4):480–490, 2011.

[43] C. N. Hunter and G. Turner. Transfer of genes-coding for apoproteins of reaction center and light-harvesting lh1 complexes to rhodobacter-sphaeroides. *Journal of General Microbiology*, 134:1471–1480, 1988.

[44] M. R. Jones, G. J. S. Fowler, L. C. D. Gibson, G. G. Grief, J. D. Olsen, W. Crielaard, and C. N. Hunter. Mutants of rhodobacter-sphaeroides lacking one or more pigment protein complexes and complementation with reaction-center, lh1, and lh2 genes. *Molecular Microbiology*, 6(9):1173–1184, 1992.

[45] M. R. Jones, R. W. Visschers, R. Vangrondelle, and C. N. Hunter. Construction and characterization of a mutant of rhodobacter-sphaeroides with the reaction center as the sole pigment protein complex. *Biochemistry*, 31(18):4458–4465, 1992.

[46] K. E. McAuley-Hecht, P. K. Fyfe, J. P. Ridge, S. M. Prince, C. N. Hunter, N. W. Isaacs, R. J. Cogdell, and M. R. Jones. Structural studies of wild-type and mutant reaction centers from

an antenna-deficient strain of rhodobacter sphaeroides: Monitoring the optical properties of the complex from bacterial cell to crystal. *Biochemistry*, 37(14):4740–4750, 1998.

[47] P. McGlynn, C. N. Hunter, and M. R. Jones. The rhodobacter-sphaeroides pufx protein is not required for photosynthetic competence in the absence of a light-harvesting system. *Febs Letters*, 349(3):349–353, 1994.

[48] L. I. Crouch, K. Holden-Dye, and M. R. Jones. Dimerisation of the rhodobacter sphaeroides rc-lh1 photosynthetic complex is not facilitated by a gxxxg motif in the pufx polypeptide. *Biochimica Et Biophysica Acta-Bioenergetics*, 1797(11):1812–1819, 1997.

[49] M. L. Groot, Ljgw van Wilderen, and M. Di Donato. Time-resolved methods in biophysics. 5. femtosecond time-resolved and dispersed infrared spectroscopy on proteins. *Photochemical Photobiological Sciences*, 6(5):501–507, 2007.

[50] Ivo H. M. van Stokkum, Delmar S. Larsen, and Rienk van Grondelle. Global and target analysis of time-resolved spectra. *Biochimica et Biophysica Acta (BBA) - Bioenergetics*, 1657(2-3):82–104, 2004.

[51] D. L. Thibodeau, E. Nabedryk, R. Hienerwadel, F. Lenz, W. Mantele, and J. Breton. Time-resolved ftir spectroscopy of quinones in rhodobacter-sphaeroides reaction centers. *Biochim Biophys Acta*, 1020(3):253–259, 1990.

[52] K. A. Bagley. Ftir studies of the d+qa and d+qb states in reaction centers from rb. sphaeroides. In M. Baltscheffsky, editor, *Current Research in Photosynthesis*, volume 1, page I.1.77–I.1.80. Kluwer Academic Publishers, Dordrecht, 1990.

[53] J. Breton, D. L. Thibodeau, C. Berthomieu, W. Mantele, A. Vermeglio, and E. Nabedryk. Probing the primary quinone environment in photosynthetic bacterial reaction centers by light-induced ftir difference spectroscopy. *Febs Letters*, 278(2):257–260, 1991.

[54] E. Nabedryk. Light-induced fourier transform infrared difference spectroscopy of the primary electron donor in photosynthetic reaction centers. In H. H. Mantsch Chapman and D., editors, *Infrared Spectroscopy of Biomolecules*, pages 39–81. Wiley-Liss, New York, 1996.

[55] W. G. Mantele, A. M. Wollenweber, E. Nabedryk, and J. Breton. Infrared spectroelectrochemistry of bacteriochlorophylls and bacteriopheophytins - implications for the binding of the pigments in the reaction center from photosynthetic bacteria. *Proceedings of the National Academy of Sciences of the United States of America*, 85(22):8468–8472, 1988.

[56] E. Nabedryk, S. Andrianambinintsoa, D. Dejonghe, and J. Breton. Ftir spectroscopy of the photoreduction of the bacteriopheophytin electron-acceptor in reaction centers of rhodobacter-sphaeroides and rhodopseudomonas-viridis. *Chem Phys*, 194(2-3):371–378, 1995.

[57] E. Nabedryk, K. A. Bagley, D. L. Thibodeau, M. Bauscher, W. Mantele, and J. Breton. A protein conformational change associated with the photoreduction of the primary and secondary quinones in the bacterial reaction center. *Febs Letters*, 266(1-2):59–62, 1990.

[58] J. Breton and E. Nabedryk. Protein-quinone interactions in the bacterial photosynthetic reaction center: Light-induced ftir difference spectroscopy of the quinone vibrations. *Biochimica Et Biophysica Acta-Bioenergetics*, 1275(1-2):84–90, 1996.

[59] L. M. Beekman, F. van Mourik, M. R. Jones, H. M. Visser, C. N. Hunter, and R. van Grondelle. Trapping kinetics in mutants of the photosynthetic purple bacterium rhodobacter sphaeroides: influence of the charge separation rate and consequences for the rate-limiting step in the light-harvesting process. *Biochemistry*, 33(11):3143–7, 1994.

[60] A. Freiberg, J. P. Allen, J. C. Williams, and N. W. Woodbury. Energy trapping and detrapping by wild type and mutant reaction centers of purple non-sulfur bacteria. *Photosynthesis Research*, 48(1-2):309–319, 1996.

[61] K. Timpmann, A. Freiberg, and V. Sundstrom. Energy trapping and detrapping in the photosynthetic bacterium rhodopseudomonas-viridis - transfer-to-trap-limited dynamics. *Chem Phys*, 194(2-3):275–283, 1995.

[62] K. Timpmann, F. G. Zhang, A. Freiberg, and V. Sundstrom. Detrapping of excitation-energy from the reaction-center in the photosynthetic purple bacterium rhodospirillum-rubrum. *Biochim Biophys Acta*, 1183(1):185–193, 1993.

[63] W. H. Xiao, S. Lin, A. K. W. Taguchi, and N. W. Woodbury. Femtosecond pump-probe analysis of energy and electron-transfer in photosynthetic membranes of rhodobacter-capsulatus. *Biochemistry*, 33(27):8313–8322, 1994.

[64] J. T. M. Kennis, T. J. Aartsma, and J. Amesz. Energy trapping in the purple sulfur bacteria chromatium-vinosum and chromatium-tepidum. *Biochimica Et Biophysica Acta-Bioenergetics*, 1188(3):278–286, 1994.

[65] J. Breton. In P. Carmona, editor, *Spectroscopy of Biological Molecules : Modern Trends*. Kluwer, The Netherlands, 1997.

[66] F. Comayras, C. Jungas, and J. Lavergne. Functional consequences of the organization of the photosynthetic apparatus in rhodobacter sphaeroides. i. quinone domains and excitation transfer in chromatophores and reaction center.antenna complexes. *J Biol Chem*, 280(12):11203–13, 2005.

[67] F. Comayras, C. Jungas, and J. Lavergne. Functional consequences of the organization of the photosynthetic apparatus in rhodobacter sphaeroides: Ii. a study of pufx- membranes. *J Biol Chem*, 280(12):11214–23, 2005.

[68] K. Gibasiewicz, M. Pajzderska, M. Ziolek, J. Karolczak, and A. Dobek. Internal electrostatic control of the primary charge separation and recombination in reaction centers from rhodobacter sphaeroides revealed by femtosecond transient absorption. *Journal of Physical Chemistry B*, 113(31):11023–11031, 2009.

[69] Chu-Kang Tang, JoAnn C. Williams, Aileen K. W. Taguchi, James P. Allen, and Neal W. Woodbury. P+ha- charge recombination reaction rate constant in rhodobacter sphaeroides reaction centers is independent of the p/p+ midpoint potentialâ . *Biochemistry*, 38(27):8794–8799, 1999.

[70] Wolfgang P. Barz, Francesco Francia, Giovanni Venturoli, B. Andrea Melandri, Andre Vermeglio, and Dieter Oesterhelt. Role of pufx protein in photosynthetic growth of rhodobacter sphaeroides. 1. pufx is required for efficient light-driven electron transfer and photophosphorylation under anaerobic conditions. *Biochemistry*, 34(46):15235–15247, 1995.

[71] Wolfgang P. Barz, Andre Vermeglio, Francesco Francia, Giovanni Venturoli, B. Andrea Melandri, and Dieter Oesterhelt. Role of the pufx protein in photosynthetic growth of rhodobacter

sphaeroides. 2. pufx is required for efficient ubiquinone/ubiquinol exchange between the reaction center qb site and the cytochrome bc1 complex. *Biochemistry*, 34(46):15248–15258, 1995.

[72] A. Vermeglio and P. Joliot. Supramolecular organisation of the photosynthetic chain in anoxygenic bacteria. *Biochimica Et Biophysica Acta-Bioenergetics*, 1555(1-3):60–64, 2002.

[73] A. Freiberg, K. Timpmann, S. Lin, and N. W. Woodbury. Exciton relaxation and transfer in the lh2 antenna network of photosynthetic bacteria. *Journal of Physical Chemistry B*, 102(52):10974–10982, 1998.

[74] M. Dezi, F. Francia, A. Mallardi, G. Colafemmina, G. Palazzo, and G. Venturoli. Stabilization of charge separation and cardiolipin confinement in antenna-reaction center complexes purified from rhodobacter sphaeroides. *Biochimica Et Biophysica Acta-Bioenergetics*, 1767(8):1041–1056, 2007.

[75] F. Francia, M. Dezi, J. Busselez, D. Levy, A. Rebecchi, A. Mallardi, G. Palazzo, B. A. Melandri, and G. Venturoli. Structural and functional analysis of the reaction center-light harvesting complex of rhodobacter sphaeroides. *Biochimica Et Biophysica Acta-Bioenergetics*, 1658:251–251, 2004.

[76] Roger C. Prince, Sandra J. G. Linkletter, and P. Leslie Dutton. The thermodynamic properties of some commonly used oxidation-reduction mediators, inhibitors and dyes, as determined by polarography. *Biochimica et Biophysica Acta (BBA) - Bioenergetics*, 635(1):132–148, 1981.

[77] R. W. Visschers, S. I. E. Vulto, M. R. Jones, R. van Grondelle, and R. Kraayenhof. Functional lh1 antenna complexes influence elec-

tron transfer in bacterial photosynthetic reaction centers. *Photosynthesis Research*, 59(1):95–104, 1999.

[78] P. L. Dutton, J. S. Leigh, and C. A. Wraight. Direct measurement of midpoint potential of primary electron-acceptor in rhodopseudomonas-spheroides in-situ and in isolated state - some relationships with ph and ortho-phenanthroline. *Febs Letters*, 36(2):169–173, 1973.

[79] S. K. Buchanan, G. C. Dismukes, and R. C. Prince. The redox potential of the primary quinone-qa of bacterial photosynthesis is independent of the divalent metal-ion. *Febs Letters*, 229(1):16–20, 1988.

[80] J. D. Olsen, G. D. Sockalingum, B. Robert, and C. N. Hunter. Modification of a hydrogen-bond to a bacteriochlorophyll-a molecule in the light-harvesting 1-antenna of rhodobacter-sphaeroides. *Proceedings of the National Academy of Sciences of the United States of America*, 91(15):7124–7128, 1994.

[81] J. D. Olsen, J. N. Sturgis, W. H. J. Westerhuis, G. J. S. Fowler, C. N. Hunter, and B. Robert. Site-directed modification of the ligands to the bacteriochlorophylls of the light-harvesting lh1 and lh2 complexes of rhodobacter sphaeroides. *Biochemistry*, 36(41):12625–12632, 1997.

[82] G. Uyeda, J. C. Williams, M. Roman, T. A. Mattioli, and J. P. Allen. The influence of hydrogen bonds on the electronic structure of light-harvesting complexes from photosynthetic bacteria. *Biochemistry*, 49(6):1146–1159.

[83] G. L. Closs, J. J. Katz, F. C. Pennington, M. R. Thomas, and H. H. Strain. Nuclear magnetic resonance spectra and molecular association of chlorophylls a and b, methyl chlorophyllides,

pheophytins, and methyl pheophorbides. *Journal of the American Chemical Society*, 85(23):3809–3821, 1963.

[84] W. Mantele, A. Wollenweber, F. Rashwan, J. Heinze, E. Nabedryk, G. Berger, and J. Breton. Fourier-transform infrared spectroelectrochemistry of the bacteriochlorophyll-a anion radical. *Photochemistry and Photobiology*, 47(3):451–455, 1988.

[85] Karlheinz Ballschmiter and Joseph J. Katz. Infrared study of chlorophyll-chlorophyll and chlorophyll-water interactions. *Journal of the American Chemical Society*, 91(10):2661–2677, 1969.

[86] D. J. Richardson, G. F. King, D. J. Kelly, A. G. McEwan, S. J. Ferguson, and J. B. Jackson. The role of auxiliary oxidants in maintaining redox balance during phototrophic growth of rhodobacter-capsulatus on propionate or butyrate. *Archives of Microbiology*, 150(2):131–137, 1988.

[87] M. R. Jones, D. J. Richardson, A. G. McEwan, S. J. Ferguson, and J. B. Jackson. Invivo redox poising of the cyclic electron-transport system of rhodobacter-capsulatus and the effects of the auxiliary oxidants, nitrate, nitrous-oxide and trimethylamine n-oxide, as revealed by multiple short flash excitation. *Biochim Biophys Acta*, 1017(3):209–216, 1990.

5.7 Supporting information: For 'Demonstration of the influence of PufX on photochemical charge separation in the reaction centre from Rhodobacter sphaeroides: An femtosecond midIR pump-probe investigation'

5.7.1 NearIR pump probe measurements on RC-LHI-X- complexes

Energy transfer and charge separation were also investigated in the near-infrared between between 750 and 950 nm, with excitation at 800 nm. Experimental information on ultrafast spectroscopy and data analysis can be found in the main text. Figure 5.7 shows EADS obtained from a global analysis of data recorded for RC-LHI-X- complexes in the presence of ascorbate and PMS. Five components were required to model the data, with lifetimes of 0.1, 1.5, 43, 292 ps and an infinite component. The first component, with a lifetime of 110 fs, might still be affected by the coherent artifact, given that its lifetime is similar to the instrument response function (∼120 fs). Hence, is not discussed any further.

The remaining EADS were dominated by the broad LH1 contribution around 885 nm. The contribution of the RC, with marker bands at 760, 800 and 867 nm was entirely overshadowed by those of the antenna. Hence, precise statements about energy transfer between the antenna and the reaction center are difficult to make. The lifetimes of the EADS were in reasonable agreement with those obtained from the mid-IR spectroscopy (see Figure 5.4, main text)

The loss of about 20% in amplitude in the 1.5 ps component around

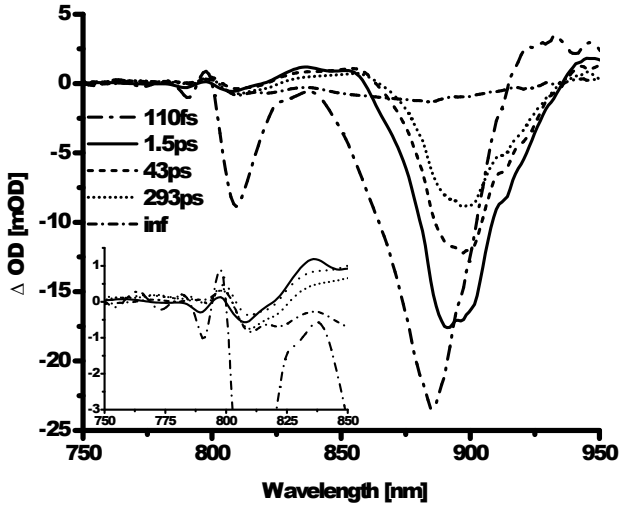

Figure 5.7: EADS obtained for RC-LHI-X- complexes after 800 nm excitation, with detection in the near-infrared.

885 nm was most likely due to exciton-exciton annihilation in the antenna ring (1), rather than transfer to the RC, which takes 20-40 ps (2, 3). Both the loss in amplitude and the lifetime are in good agreement with what was found in the mid-IR.

The relative large size of the LH1 signals compared to those of the RC and the amplitude of the final spectrum, has been observed before for this kind of system and can be explained by excitonic interactions of the BChls arranged in a packed circular symmetric structure (4–6). In brief, due to the collective nature of the initial excitation, absorption of one photon by the antenna can lead to an absorbance difference signal with a magnitude which corresponds to the bleaching of several monomeric BChl molecules (2).

The 43 ps and 293 ps spectra were very similar in the antenna

region, apart from another 20% loss in amplitude. In the RC region between 750-850 nm, the 800 nm bandshift signal typical for P^+ formation (7)) can be identified, and the EADS of the final component for RC-LH1-X- complexes resembled that of isolated RCs quite well (Fig 5.8). However, it is clear that in the midIR the spectral features associated with LH1 and the RC are more balanced in amplitude, richer in detail and provide therefore a more valuable tool for following the electron transfer process in the RC in the presence of LH1.

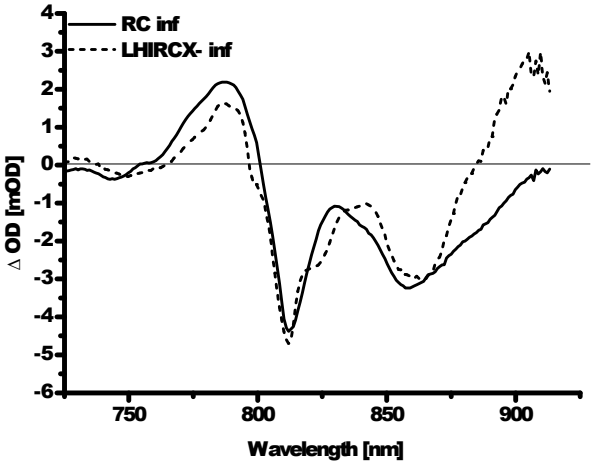

Figure 5.8: EADS of the final component for the RC and RC-LH1-X- complex.

Bibliography

[1] A. Freiberg, K. Timpmann, S. Lin, and N. W. Woodbury. Exciton relaxation and transfer in the lh2 antenna network of photosynthetic bacteria. *Journal of Physical Chemistry B*, 102(52):10974–10982, 1998.

[2] J. T. M. Kennis, T. J. Aartsma, and J. Amesz. Energy trapping in the purple sulfur bacteria chromatium-vinosum and chromatium-tepidum. *Biochimica Et Biophysica Acta-Bioenergetics*, 1188(3):278–286, 1994.

[3] V. Nagarajan and W. W. Parson. Excitation energy transfer between the b850 and b875 antenna complexes of rhodobacter sphaeroides. *Biochemistry*, 36(8):2300–2306, 1997.

[4] M. Dahlbom, T. Pullerits, S. Mukamel, and V. Sandstrom. Exciton delocalization in the b850 light-harvesting complex: Comparison of different measures. *Journal of Physical Chemistry B*, 105(23):5515–5524, 2001.

[5] V. Novoderezhkin, R. Monshouwer, and R. van Grondelle. Disordered exciton model for the core light-harvesting antenna of rhodopseudomonas viridis. *Biophysical Journal*, 77(2):666–681, 1999.

[6] V. I. Novoderezhkin and A. P. Razjivin. The study of delocalized states in the antenna of purple bacteria by nonlinear spectroscopy. *Biofizika*, 42(1):164–168, 1997.

[7] W. Zinth and J. Wachtveitl. The first picoseconds in bacterial photosynthesis–ultrafast electron transfer for the efficient conversion of light energy. *Chemphyschem*, 6(5):871–80, 2005.